Hindawi
International Journal of Photoenergy
Volume 2019, Article ID 3725364, 10 pages
https://doi.org/10.1155/2019/3725364

Research Article

Experimental Investigation on a Thermoelectric Cooler for Thermal Management of a Lithium-Ion Battery Module

Xinxi Li, Zhaoda Zhong, Jinghai Luo, Ziyuan Wang, Weizhong Yuan, Guoqing Zhang, Chengzhao Yang, and Chuxiong Yang

School of Materials and Energy, Guangdong University of Technology, Guangzhou 510006, China

Correspondence should be addressed to Xinxi Li; pkdlxx@163.com

Received 29 August 2018; Accepted 16 October 2018; Published 11 February 2019

Academic Editor: Joaquim Carneiro

Electric vehicles (EVs) powered by lithium batteries, which are a promising type of green transportation, have attracted much attention in recent years. In this study, a thermoelectric generator (TEG) coupled with forced convection (F-C) was designed as an effective and feasible cooling system for a battery thermal management system. A comparison of natural convection cooling, F-C cooling, and TEG cooling reveals that the TEG is the best cooling system. Specifically, this system can decrease the temperature by 16.44% at the discharge rate of 3C. The coupled TEG and F-C cooling system can significantly control temperature at a relatively high discharge rate. This system not only can decrease the temperature of the battery module promptly but also can reduce the energy consumption compared with the two other TEG-based cooling systems. These results are expected to supply an effective basis of the design and optimization of battery thermal management systems to improve the reliability and safety performance of EVs.

1. Introduction

The rapid development of global industrialization has increased the greenhouse gas emissions and nonrenewable energy shortage, which are urgent concerns for the entire society [1, 2]. To effectively address serious environmental problems, pure electric vehicles (EVs) and hybrid EVs as green power equipment and environment-friendly transport tools compared to traditional diesel locomotives are developed [3–6]. Lithium-ion batteries have many advantages, such as high power density, high energy density, long lifetime, and less self-discharge; they play an important role in the fields of EV and energy storage station [7–10]. However, lithium-ion batteries overheat during operation, which seriously hinders their application in EV/HEV [11, 12]. In particular, the battery module exhibits a potential safety hazard under a high-temperature environment, thereby shortening the battery lifespan [13]. Lithium batteries are easily overheated by rapid discharging, overcharging, and excessive environmental heating in practical application, thereby leading to serious disasters, such as firing and explosion accident [14, 15]. Therefore, given that the kinetic and transport processes depend seriously on the temperature, thermal management of a battery module is necessary. This way maintains the battery module within a certain safety range and prevents thermal runaway. Consequently, a thermal management system which satisfies an operational temperature range should be proposed to enable normal application for a battery module. Such system requires cooling preservation to prolong the lifetime of batteries in the module.

Various battery thermal management systems (BTMS) have been widely installed on HEVs and EVs [16–21]. During the repeated charging and discharging process, the battery module would generate a large amount of heat, especially at a relatively high rate [22, 23]. The BTMS can avoid the rapid increase in temperature when the battery module is maintained at high temperature during a long time in some remote regions. Increasing the corresponding auxiliary equipment to maintain the battery module at proper temperature is the best solution for HEVs and EVs. Meng et al. [24] utilized the refrigeration system to cool a lead acid-based

battery cabinet. The flow field and temperature distribution of two- and six-layer configurations containing 24 batteries were analyzed in detail by experiments and numerical simulations. The results showed that the passive air cooling system utilizing natural convection (N-C) can maintain battery temperature at optimal values between 20°C and 30°C. Situ et al. [25] designed a coupled battery thermal management (BTM) system based on a novel quaternary phase change material plate for balancing the temperature in rectangular $LiFePO_4$ battery modules; meanwhile, the paraffin, expanded graphite, low-density polyethylene, and copper mesh were combined into a quaternary PCMP to strengthen the heat transfer. The results revealed that the double outstretched copper mesh through the phase change material plate could disturb the air flow tempestuously and give rise to a decrease in thermal resistance; thus, the temperature distribution inside the battery and temperature uniformity within the battery module were both better optimized. However, the battery module cannot be applied during the operating status because the batteries have to continue working at a hot environment. The stability, reliability, and simplification of the system need to be improved for fixed investment and power consumption. Long-term safety preservation of battery temperature is also important.

In recent years, the thermoelectric effect in a semiconductor has been widely investigated because it can produce temperature gradient when an electric current is launched. And thermoelectric generator (TEG) cooling can promptly create a relatively lower temperature than the surrounding temperature, which could not need extra moving parts for converting electrical capacity into refrigerating capacity. The degree of cooling can easily be adjusted depending on the current size. The refrigeration effect can also be maintained for a long time without extra maintenance. This characteristic not only can improve the system reliability but also can simplify the system structure for thermal management. Therefore, thermoelectric generator (TEG) cooling is an effective approach for thermal management of a battery module [26, 27].

To overcome the negative effects of heat dissipation, considerable efforts have been invested to investigate an effective cooling system for a battery module, according to the heat transfer medium, which should include the air-based thermal management systems such as natural or air-forced cooling [28, 29], liquid-based thermal management systems such as heat pipe or fluid liquid cooling [30, 31], and phase change material-based thermal management system [32, 33]. However, air-based thermal management systems would hinder the heat dissipation among the batteries due to their relatively low thermal conductivity and heat transferring efficiency. Meanwhile, the liquid-based thermal management systems with complex structures have to increase the extra cost, which also easily causes short circuit if leakage of the liquid occurs in the system and leads to serious thermal runaway problem for the battery module. In addition, a phase change material-based thermal management system has to affect the weight of battery module increment and its cost is extremely high [34]. The instant performance of heat dissipation is also challenging.

In this study, a new thermal management model of a temperature control battery based on semiconductor refrigeration is proposed. This model is characterized by the real-time feedback of the temperature of the battery module through the rapid cooling/heating of the semiconductor and the effect of the fan. The temperature control module is reflected in the temperature control heat management model by the temperature control module of the battery protection board. The design and specific operation of the experiment are as follows. First, adiabatic cotton is used to wrap the experiment box to create an adiabatic environment. Then, the parameters of the temperature control module are fully tested. Finally, the discharge experiments of the battery module at different rates and conditions are tested.

2. Materials

2.1. Working Principles. Lithium-ion batteries produce a large amount of heat with the electrochemical reaction during charging and discharging. Specifically, the battery module causes the sharp increase in temperature at a high discharge rate. The heat production of a lithium-ion battery during charging and discharging is mainly composed of four parts, which can be found in

$$Q = Q_r + Q_j + Q_p + Q_s, \tag{1}$$

where Q is the actual generated heat of the battery, Q_r is the reaction heat, Q_j is the Joule heat, Q_p is the reaction heat in the electrode, and Q_s is the secondary reaction heat.

The principles of the TEG are the Seebeck and Peltier effects. The Seebeck effect, which was discovered in 1821, is a phenomenon due to the difference in temperature between two substances or semiconductors. This difference causes the voltage difference between the two substances. The aforementioned effect can be expressed as

$$\alpha = \frac{\Delta V}{\Delta T}, \tag{2}$$

where α is the Seebeck coefficient, $\triangle V$ is the voltage difference, and $\triangle T$ is the temperature difference.

The Peltier effect, which was discovered in 1834, is a phenomenon when the current passes through the different substances, which results in decalescence and exothermic reaction at the joint of the different substances with the direction of the current in addition to the irreversible Joule heat. TEG materials are evaluated by the merit ZT, which is defined on the basis of N- and P-type material properties and is determined by three physical properties, namely, Seebeck coefficient, electrical conductivity, and thermal conductivity. These properties can be found in

$$\mathrm{ZT} = \frac{\alpha^2}{\kappa}\sigma T, \tag{3}$$

where κ is the thermal conductivity, σ is the electrical conductivity, and T is the temperature.

The conversion efficiency between electrical power and refrigeration is measured using the coefficient of performance (COP) in the TEG, which can be expressed as

$$\mathrm{COP} = \frac{Q_c}{P_{\mathrm{input}}}, \tag{4}$$

where Q_c is the refrigerating capacity and P_{input} is the electric power input. Obviously, the better the ZT, the higher the COP. The optimum refrigeration effectiveness for ideal assembly equipment is presented as follows [35]:

$$\mathrm{COP}_{\max} = \frac{T_H - T_C}{T_H} \frac{\sqrt{1+\mathrm{ZT}} - 1}{\sqrt{1+\mathrm{ZT}} + (T_C/T_H)}, \tag{5}$$

where T_H is the temperature of the hot end and T_C is the temperature of the cold end.

2.2. Semiconductor and Battery. The physical parameters of the different commercial chips include the maximum current, the maximum voltage, the maximum temperature difference, and the maximum refrigerating capacity, which are displayed in Table 1. The maximum refrigerating capacity and the operated current and voltage should be comprehensively considered. Thus, the TEC1-12706-type chip is the best choice.

The lithium-ion battery type in this research is 18650, and its capacity and standard voltage are 2200–3200 mAh and 3.7 V, respectively.

2.3. Design. In this research, a new thermal management model of a temperature control battery based on semiconductor refrigeration was developed. The following parts present the detailed description of the experimental platform.

Firstly, the battery module was constructed by nine 18650-type batteries, which were arranged with a 3×3 series connection. Figure 1(a) shows the 3D configuration diagram of the battery module. The battery module consisted of a nut, a battery box, a state fixed bolt, and nine batteries in series. T-type thermocouples were applied to measure the temperature of each battery in the module, which were adhered to the surface of the battery. Figure 1(b) shows the sectional view. For example, the numbers 1, 4, and 5 in Figure 1(b), which are the measurement points of the corresponding batteries in the module, are noted as T1, T4, and T5, respectively.

Secondly, the TEG was constructed with TEC1-12706, fins, and fans, as shown in Figure 2. Figure 2(a) shows the photograph of the refrigeration equipment. The experimental equipment was wrapped with the 2 mm insulated cotton package to form an adiabatic environment in an acrylic box. Figure 2(b) shows the photo of the battery module in this experiment. The upper section of the equipment comprised the top part of the fan and the hot portion of the TEG, as shown in Figure 2(c). The lower section of the equipment comprised the bottom part of the fan and the cold portion of the TEG, as shown in Figure 2(d). The semiconductor chip was located between the upper and lower sections.

Table 1: Performance parameters of commercial TEG.

Type	$I_{\max}$ (A)	$U_{\max}$ (V)	$\triangle T_{\max}$ (°C)	Q_{cmax} (W)	$L \times W \times H$ (mm)
TEC1-12703	3.0	15.4	67	31.1	$40 \times 40 \times 4.5$
TEC1-12704	4.0	15.4	67	39.3	$30 \times 30 \times 4.2$
TEC1-12705	5.0	15.4	67	49.4	$40 \times 40 \times 3.9$
TEC1-12706	6.0	15.4	67	55.0	$40 \times 40 \times 3.8$
TEC1-12707	7.0	15.4	67	66.3	$40 \times 40 \times 3.7$
TEC1-12708	8.0	15.4	67	75.8	$40 \times 40 \times 3.6$

Figure 3 displays the experimental platform. The battery module was composed of 3×3 series 18650 batteries. The standard voltage of the integrity module was 3.7 V, the current was 19.8 A, and the capacity was 8.8 Ah. The semiconductor chip was TEC1-12706, and the working voltage and current were 12 V and 6 A, respectively. The temperature control device was set to 40°C. When the temperature of the battery module during charging and discharging reached 40°C, the TEG would enter the working states. Under different discharge rates of the battery module such as 1, 1.5, 2, 2.5, and 3 C, the thermal management system based on the thermoelectric effect was analyzed in detail and compared with N-C cooling and forced convection (F-C) cooling conditions.

Overall, the temperature of the battery module could be controlled using the TEG and the fan, and the temperature of different batteries in the module could be managed uniformly. Therefore, on the basis of the thermoelectric and forced-air cooling effects, the temperature of the battery module would be adjusted within the safety range.

3. Result and Discussion

The following sections present the proposed experiment results and analysis. Section 3.1 shows the schematic of the battery module with coupled TEG and F-C. Section 3.2 shows the experimental results of TEG cooling, N-C cooling, and F-C cooling at different rates of the battery module. Section 3.3 shows the optimizing results of the semiconductor heat management device.

3.1. Schematic of the Battery Module with Coupled TEG and F-C. Figure 4 shows that the TEG is composed of a P semiconductor and N semiconductor; the double surface sides of which are adhered with a specific ceramic sheet with high thermal conductivity and excellent insulation properties. When the current flows from N to P under the Peltier effect, the refrigeration process occurs on the ceramic sheet. On the contrary, when the current flows from P to N, the exothermic effect occurs on the fins. The TEG can effectively convert electric energy into heat energy when direct current power is launched. In this equipment, the TEG adjacent to the batteries can convey the heat produced by the battery module to the other side. This way can control and balance the temperature of the battery module to avoid serious accidents.

Figure 5 shows that, when the direct current is switched on, the temperature is changed dramatically at less than

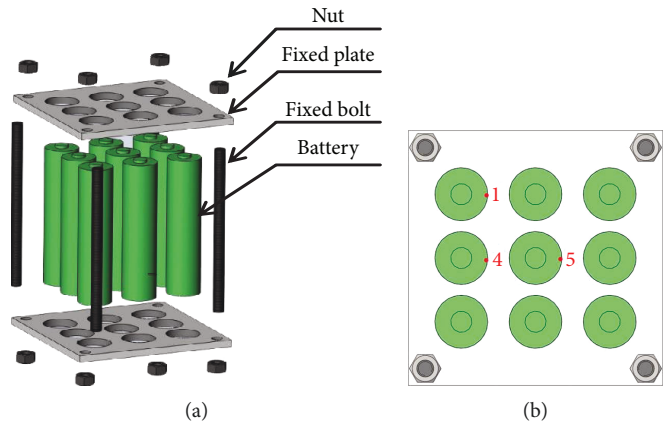

Figure 1: 3D diagram of the battery module and the temperature measurement points of the battery module: (a) 3D diagram of the battery module and (b) the position of temperature measurement points.

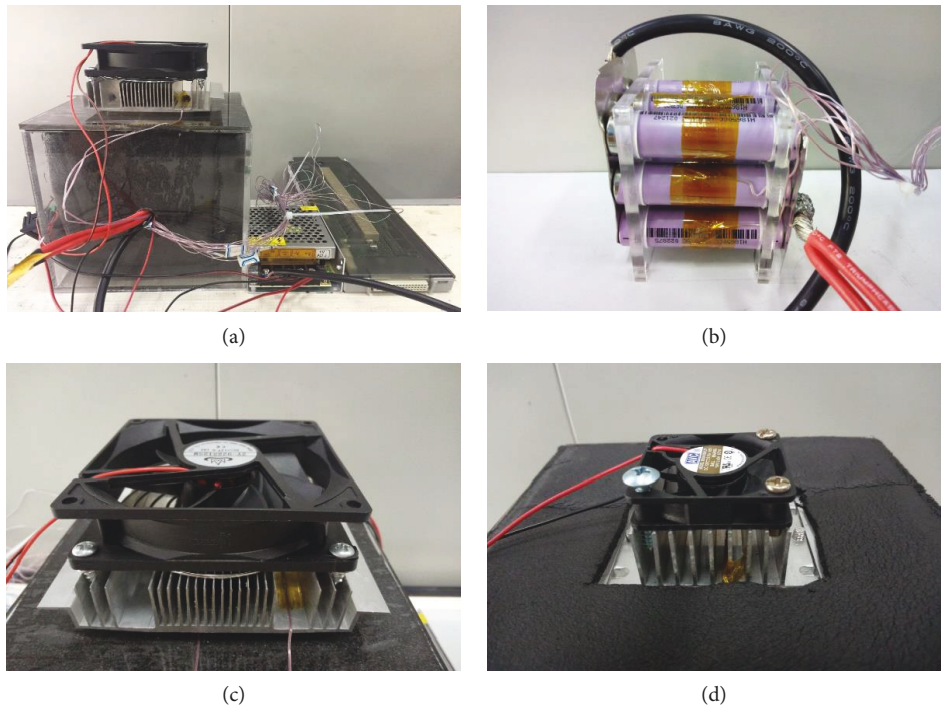

Figure 2: Physical and local diagrams of the experiment: (a) the whole experiment equipment, (b) the battery module, (c) the thermoelectric generators, and (d) the semiconductor chip between the upper and lower sections.

5 min on both sides of the TEG. In the refrigeration section, the temperature drops rapidly from 28.82°C to 9.56°C. On the contrary, the temperature increases quickly from 29.01°C to 41.03°C on the exothermic section.

After 5 min, the temperature changes slowly in the TEG. The ultimate temperature is 4.71°C on the refrigeration section and is 41.22°C on the exothermic section. This phenomenon is due to two main reasons. On the one hand, the current flows through the P semiconductor and N semiconductor, thereby causing temperature difference in accordance with the Peltier effect. On the other hand, the temperature transfers through the ceramic material, thus increasing the temperature on both sides of the TEG to achieve new balance.

3.2. Experimental Results of the TEG, N-C, and F-C Cooling at Different Rates of a Battery Module. Figure 6 shows the temperature of nine batteries in the module accompanied with different cooling models such as TEG, F-C, and N-C at various discharge rates. The temperature of the middle battery in the module is slightly higher than those of other batteries. The main reason is ascribed to the superposition of other nearby batteries. As shown in Figures 6(a) and 6(b), the temperatures of the battery module with F-C increase slower than those of the module with N-C. The main reason is that F-C accelerates the air flow velocity and thus improves the capacity of dissipating heat. As shown in Figure 6(c), the temperature of the module with TEG not only presents decreasing tendency but also shows lower values than those

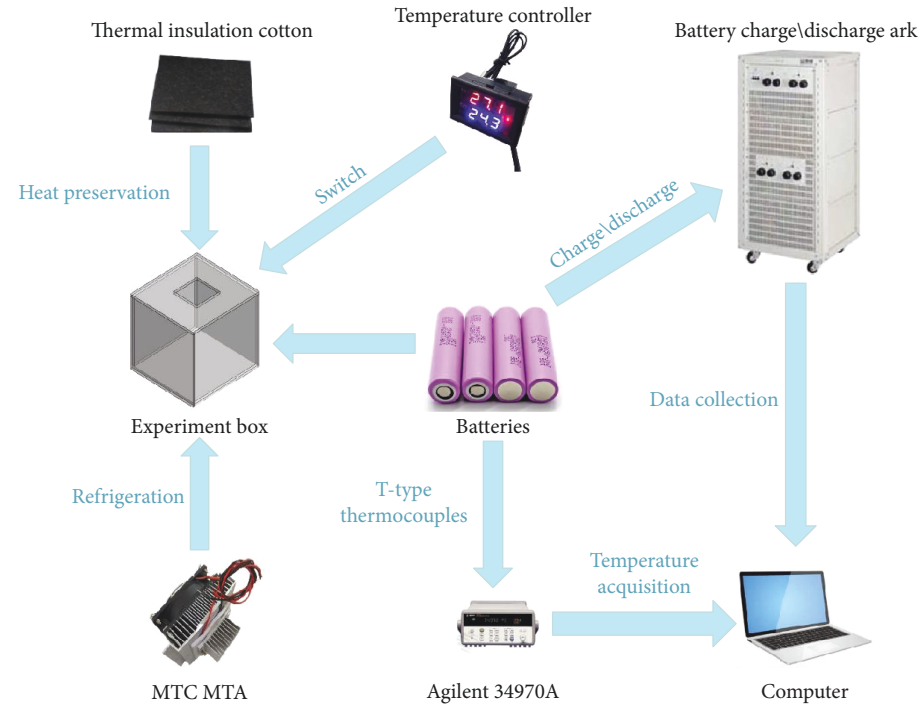

Figure 3: Schematic of the thermal response measurement platform used for batteries.

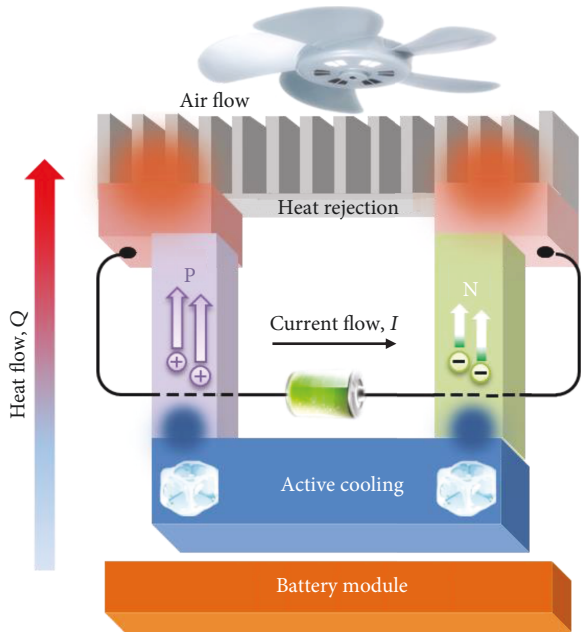

Figure 4: Schematic of the battery module with coupled TEG and F-C.

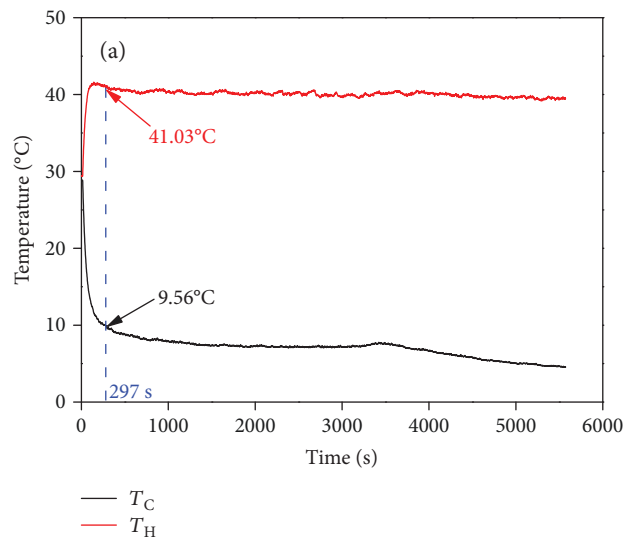

Figure 5: Temperature and time diagram of the cold and hot ends of TEG refrigeration.

of other cooling models as time progresses during discharging at 1 C. This finding may be because the TEG is accompanied by refrigerating capacity adjacent to the battery module in the equipment. The interchange with the heat produced by the battery decreases the temperature to protect the safety of the battery module. What is more, at high discharging rate conditions, the average temperature of the TEG cooling model is still lower than those of the F-C and N-C cooling models.

In Figure 7(a), it shows that the temperature of the battery module increases rapidly as the discharge rate increases. After analyzing the results of three duplicate experiments, Figure 7(b) shows the average value of the maximum temperatures of the battery module with the N-C, F-C, and TEG cooling models at different discharge rates and the standard deviation is indicated by error bars. Table 2 shows the exact value of the temperatures.

Notably, the TEG cooling model considerably reduces the temperature regardless of the discharge rate. The temperature differences among the batteries in the module are also

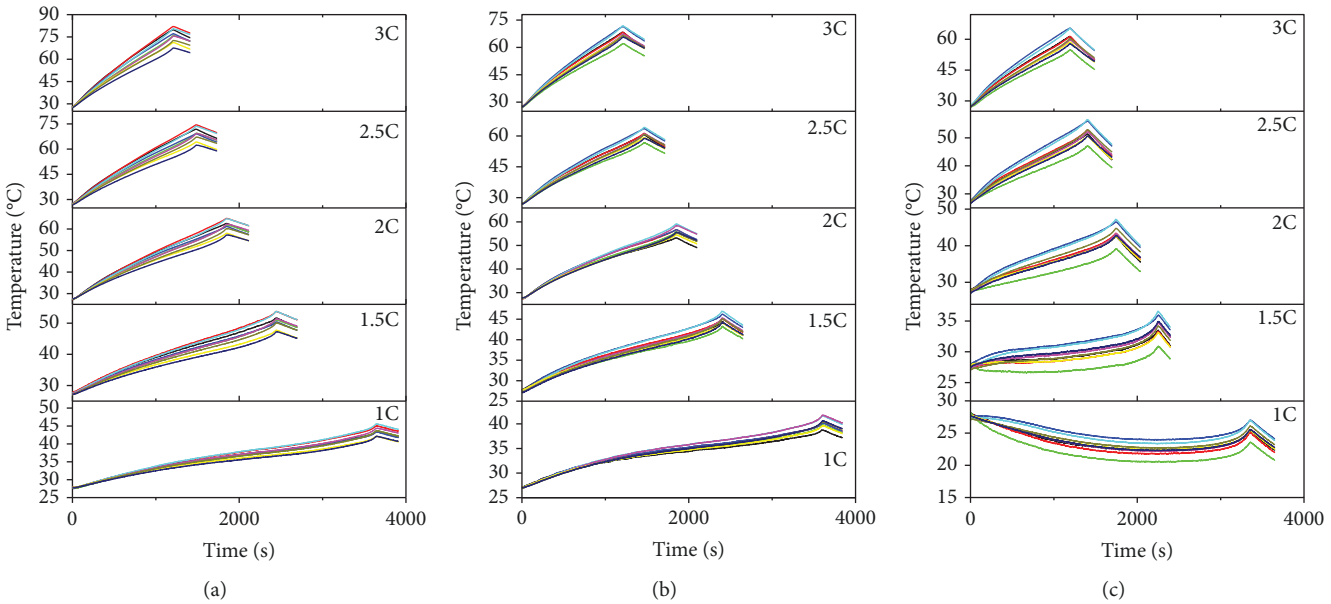

Figure 6: Temperature and time diagram of N-C, F-C, and TEG cooling thermal management at different discharge rates of batteries: (a) N-C cooling, (b) N-C cooling, and (c) TEG cooling.

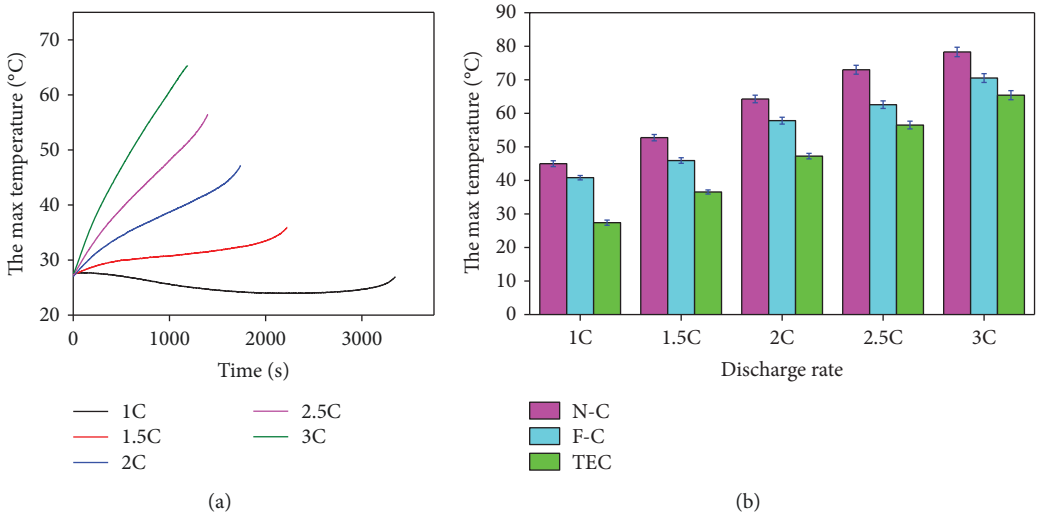

Figure 7: Diagram of the highest channel at different rates: (a) temperature variations as time changes and (b) the column graphs with the maximum temperature of N-C, F-C, and TEG.

Table 2: Exact value of the temperatures of N-C, F-C, and TEG cooling models.

Rate	1C	1.5C	2C	2.5C	3C
N-C	44.98	52.74	64.28	72.99	78.30
F-C	40.81	45.91	57.82	62.58	70.52
TEG	27.40	35.56	47.24	56.52	65.43

reduced, which reveals that the TEG cooling model can effectively balance the temperatures in the module. Therefore, the TEG is an effective method to control and balance the temperature of the battery module. This method not only can promptly decrease the temperature's increasing speed but also can remarkably reduce the temperature value.

3.3. Optimization of the Semiconductor Heat Management Device. Figure 8 shows the battery module with the coupled TEG and F-C cooling system. In a facial working condition, the thermal management for the battery module must be conducted when the temperature is higher than 40°C. In this study, three cooling systems, namely, pure TEG, F-C coupled with TEG at 40°C (FC+TEG-40°C), and TEG coupled with F-C both at 40°C (FC-40°C+TEG-40°C), were compared to analyze the cooling performance. In the FC+TEG-40°C cooling system, the fans for F-C were continued to operate

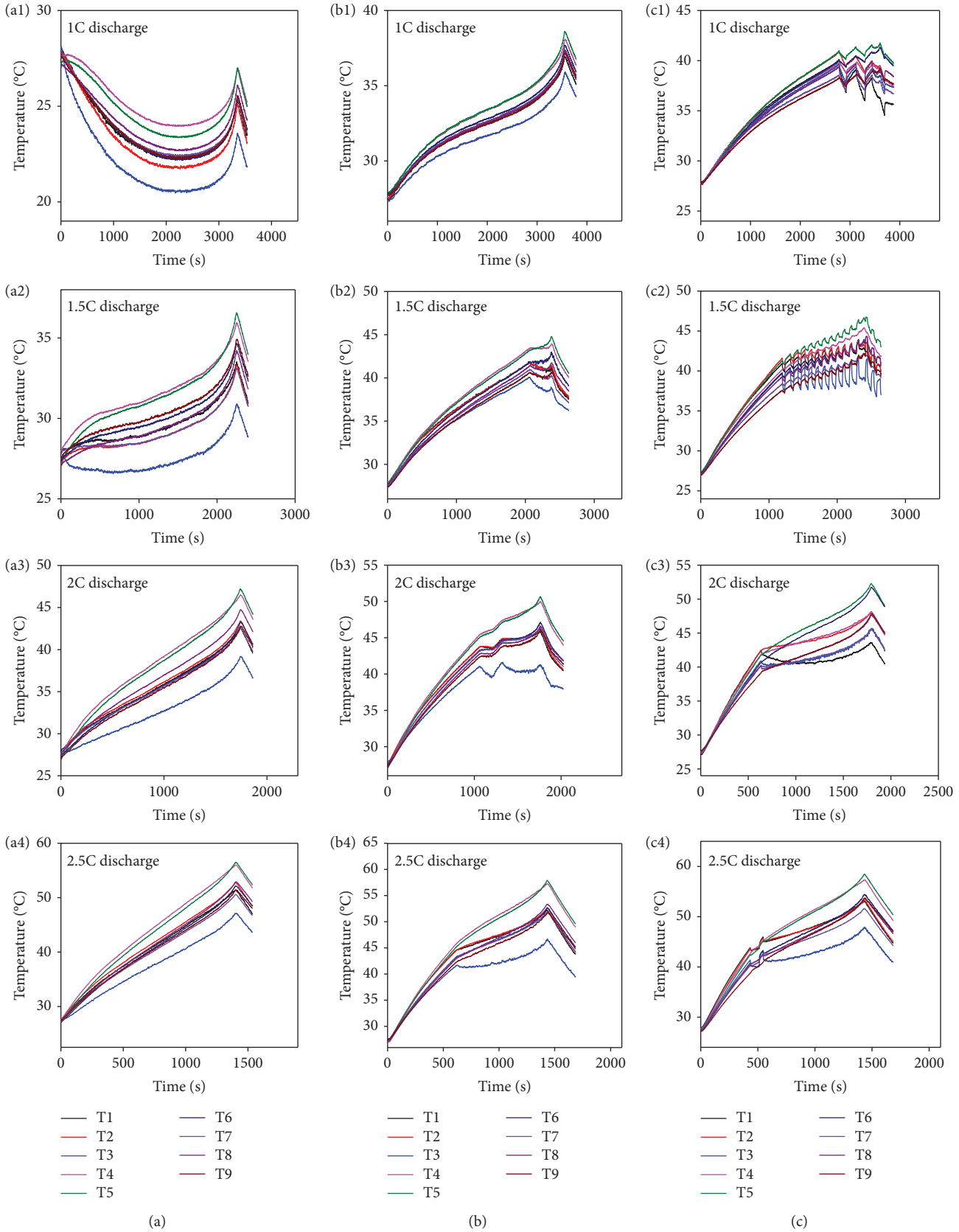

Figure 8: Thermal management model of TEG temperature control in different modes: (a) single TEG, (b) FC+TEG-40°C, and (c) FC-40°C+TEG-40°C.

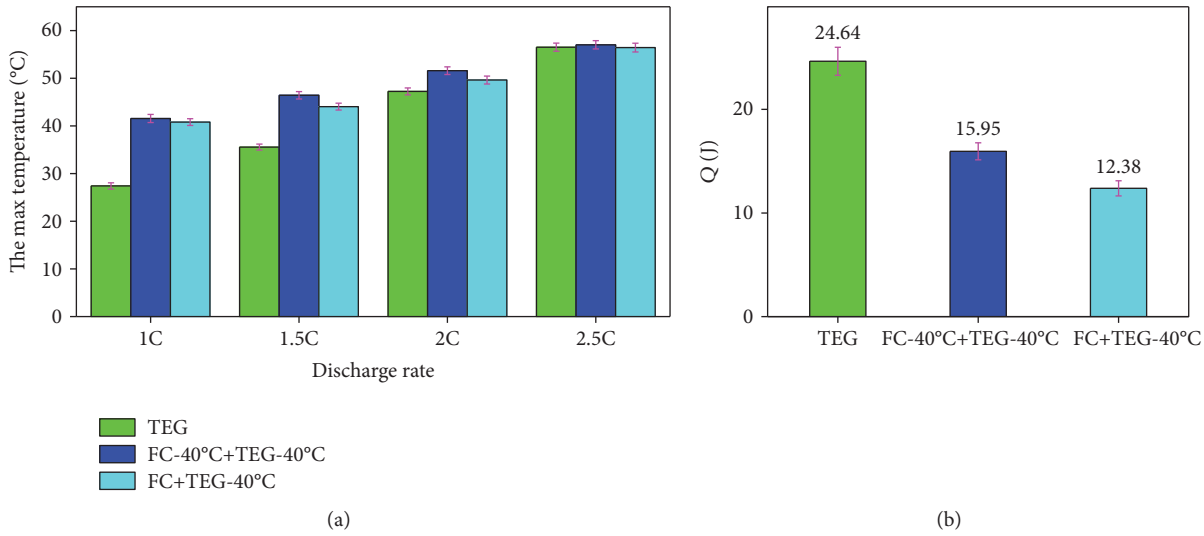

Figure 9: The maximum temperature and energy consumption among pure TEG, FC+TEG-40°C, and FC-40°C+TEG-40°C: (a) column graphs with the maximum temperature TEG, FC+TEG-40°C, and FC-40°C+TEG-40°C and (b) the diagram of energy consumption.

at all periods and the TEG for thermoelectric refrigeration was launched at the average temperature of the battery module of 40°C.

In the FC-40°C+TEG-40°C cooling system, the TEG for thermoelectric refrigeration and the fans for F-C were launched at the average temperature of the battery module of 40°C. The temperature of the three cooling systems was measured at the discharge rates of 1.0, 1.5, 2.0, and 2.5 C as time progressed. The results show that the pure TEG cooling system presents excellent cooling performance. Specifically, the corresponding temperatures of this system are lower than those of the two other cooling systems. The reason is that the TEG for thermoelectric refrigeration can effectively provide a cooling resource to exchange the heat produced by the battery module. FC-40°C+TEG-40°C displays a relatively high temperature, but it still can satisfy the requirements of the temperature of the battery module in application at the discharge rate of 2.5 C.

After analyzing the results of the three duplicate experiments, the average value of the maximum temperatures among the pure TEG, FC+TEG-40°C, and FC-40°C+TEG-40°C is shown in Figure 9(a) and the standard deviation is indicated by error bars. Meanwhile, Table 3 shows the corresponding average value of the maximum temperatures.

Figure 9(b) shows the energy consumption for comparing the economic cost, and the error bars indicate one standard deviation of the energy consumption, which is calculated by multiplying the current, voltage, and time during the three duplicate experiment processes. Using the formula $Q = U \cdot I \cdot t$, the pure TEG is found to exhibit the highest energy waste during refrigeration compared with the two other systems. On the contrary, FC+TEG-40°C consumes the least energy. Thus, FC+TEG-40°C is the best choice as the thermal management model of TEG temperature control.

Table 3: Corresponding temperature value of the pure TEG, FC+TEG-40°C, and FC-40°C+TEG-40°C.

Rate	1C	1.5C	2C	2.5C
TEG	27.40	35.56	47.24	56.52
FC+TEG-40°C	41.56	46.63	51.59	57.02
FC-40°C+TEG-40°C	40.81	44.05	49.63	56.43

4. Conclusions

In this study, the thermal management system for a cylindrical lithium-ion battery module constructed by nine 18650-type batteries was designed and compared with traditional air cooling systems, which was based on semiconductor thermoelectric cooling, natural forced cooling, and forced convection cooling. The maximum temperature rise and distribution within the different battery modules at different discharge rates were investigated by experiment. The maximum temperature of thermal management based on the TEG cooling system was optimized. And three cooling systems which were pure TEG, F-C coupled with TEG at 40°C (FC+TEG-40°C), and TEG coupled with F-C both at 40°C (FC-40°C+TEG-40°C) were compared to further analyze the cooling performance. The main conclusions are summarized as follows:

(1) The temperature of the battery module with a TEG presented a decreasing tendency and lower values than F-C and N-C cooling models as time progresses during discharging at 1 C. The main reason was that the TEG accompanied by refrigerating capacity adjacent to the battery module in the equipment can interchange the heat produced by the battery for decreasing the temperature of the batteries

(2) The temperature can be controlled by a TEG cooling system for a battery module. At the discharge rate of 3 C, the highest temperature is 65.43°C, which is lower than those of the F-C cooling model (70.52°C) and the N-C cooling model (78.30°C). Thus, the TEG is an effective method to control and balance the temperature for a battery module. This method not only can promptly decrease the temperature's increasing speed but also can considerably reduce the temperature value

(3) The pure TEG cooling system presented excellent cooling performance among the pure TEG, FC+TEG-40°C, and FC-40°C+TEG-40°C cooling models; however, it exhibited the highest energy waste during refrigeration compared with the two other systems. Considering the energy consumption and controlling temperature performance, the FC+TEG-40°C cooling model was the best choice as a thermal management system for a battery module

In the future work, the TEG preheating and waste heat recovery performance in a cold environment would be investigated to improve the thermal performance and adjust the operating temperature range of a battery module. It would play an important role in prolonging the battery lifespan and enhancing the battery safety performance.

Data Availability

The original data used to support the findings of this study are included within the article. The table data used to support the findings of this study are available from the corresponding author upon request.

Conflicts of Interest

The authors declare that they have no conflicts of interest.

Acknowledgments

This work is supported by the South Wisdom Valley Innovative Research Team Program (2015CXTD07) and the Science and Technology Application Research and Development Projects of Guangdong Province, China (2015B010135010).

References

[1] M. D. Yang, M. D. Lin, Y. H. Lin, and K. T. Tsai, "Multiobjective optimization design of green building envelope material using a non-dominated sorting genetic algorithm," *Applied Thermal Engineering*, vol. 111, pp. 1255–1264, 2017.

[2] M. J. Zhang, M. H. Qin, C. Rode, and Z. Chen, "Moisture buffering phenomenon and its impact on building energy consumption," *Applied Thermal Engineering*, vol. 124, pp. 337–345, 2017.

[3] W. X. Wu, X. Q. Yang, G. Q. Zhang, K. Chen, and S. F. Wang, "Experimental investigation on the thermal performance of heat pipe-assisted phase change material based battery thermal management system," *Energy Conversion and Management*, vol. 138, pp. 486–492, 2017.

[4] Y. H. Ren, Z. Q. Yu, and G. J. Song, "Thermal management of a Li-ion battery pack employing water evaporation," *Journal of Power Sources*, vol. 360, pp. 166–171, 2017.

[5] M. F. M. Sabri, K. A. Danapalasingam, and M. F. Rahmat, "A review on hybrid electric vehicles architecture and energy management strategies," *Renewable and Sustainable Energy Reviews*, vol. 53, pp. 1433–1442, 2016.

[6] S. Zhang, R. Xiong, and J. Cao, "Battery durability and longevity based power management for plug-in hybrid electric vehicle with hybrid energy storage system," *Applied Energy*, vol. 179, pp. 316–328, 2016.

[7] S. K. Mohammadian, Y. L. He, and Y. Zhang, "Internal cooling of a lithium-ion battery using electrolyte as coolant through microchannels embedded inside the electrodes," *Journal of Power Sources*, vol. 293, pp. 458–466, 2015.

[8] P. K. Nayak, L. Yang, W. Brehm, and P. Adelhelm, "From lithium-ion to sodium-ion batteries: advantages, challenges, and surprises," *Angewandte Chemie International Edition*, vol. 57, no. 1, pp. 102–120, 2018.

[9] S. Abada, G. Marlair, A. Lecocq, M. Petit, V. Sauvant-Moynot, and F. Huet, "Safety focused modeling of lithium-ion batteries: a review," *Journal of Power Sources*, vol. 306, pp. 178–192, 2016.

[10] H. Qu, X. Lu, and M. Skorobogatiy, "All-solid flexible fiber-shaped lithium ion batteries," *Journal of the Electrochemical Society*, vol. 165, no. 3, pp. A688–A695, 2018.

[11] G. Jiang, J. Huang, Y. Fu, M. Cao, and M. Liu, "Thermal optimization of composite phase change material/expanded graphite for Li-ion battery thermal management," *Applied Thermal Engineering*, vol. 108, pp. 1119–1125, 2016.

[12] N. Javani, I. Dincer, G. F. Naterer, and B. S. Yilbas, "Heat transfer and thermal management with PCMs in a Li-ion battery cell for electric vehicles," *International Journal of Heat and Mass Transfer*, vol. 72, pp. 690–703, 2014.

[13] H. Fathabadi, "High thermal performance lithium-ion battery pack including hybrid active–passive thermal management system for using in hybrid/electric vehicles," *Energy*, vol. 70, pp. 529–538, 2014.

[14] W. Wu, X. Yang, G. Zhang et al., "An experimental study of thermal management system using copper mesh-enhanced composite phase change materials for power battery pack," *Energy*, vol. 113, pp. 909–916, 2016.

[15] B. Mortazavi, H. Yang, F. Mohebbi, G. Cuniberti, and T. Rabczuk, "Graphene or h-BN paraffin composite structures for the thermal management of Li-ion batteries: a multiscale investigation," *Applied Energy*, vol. 202, pp. 323–334, 2017.

[16] Z. J. An, L. Jia, Y. Ding, C. Dang, and X. J. Li, "A review on lithium-ion power battery thermal management technologies and thermal safety," *Journal of Thermal Science*, vol. 26, no. 5, pp. 391–412, 2017.

[17] G. Xia, L. Cao, and G. Bi, "A review on battery thermal management in electric vehicle application," *Journal of Power Sources*, vol. 367, pp. 90–105, 2017.

[18] Z. Rao, Z. Qian, Y. Kuang, and Y. Li, "Thermal performance of liquid cooling based thermal management system for cylindrical lithium-ion battery module with variable contact surface," *Applied Thermal Engineering*, vol. 123, pp. 1514–1522, 2017.

[19] K. Chen, M. Song, W. Wei, and S. F. Wang, "Structure optimization of parallel air-cooled battery thermal management system with U-type flow for cooling efficiency improvement," *Energy*, vol. 145, pp. 603–613, 2018.

[20] M. Al-Zareer, I. Dincer, and M. A. Rosen, "Electrochemical modeling and performance evaluation of a new ammonia-based battery thermal management system for electric and hybrid electric vehicles," *Electrochimica Acta*, vol. 247, pp. 171–182, 2017.

[21] M. Al-Zareer, I. Dincer, and M. A. Rosen, "Novel thermal management system using boiling cooling for high-powered lithium-ion battery packs for hybrid electric vehicles," *Journal of Power Sources*, vol. 363, pp. 291–303, 2017.

[22] M. Chen, F. Bai, W. Song et al., "A multilayer electro-thermal model of pouch battery during normal discharge and internal short circuit process," *Applied Thermal Engineering*, vol. 120, pp. 506–516, 2017.

[23] W. Song, M. Chen, F. Bai, S. Lin, Y. Chen, and Z. Feng, "Non-uniform effect on the thermal/aging performance of lithium-ion pouch battery," *Applied Thermal Engineering*, vol. 128, pp. 1165–1174, 2018.

[24] X. Z. Meng, Z. Lu, L. J. Su et al., "Numerical and experimental investigation on thermal management of an outdoor battery cabinet," in *ASME 2014 International Mechanical Engineering Congress and Exposition*, 10 pages, Montreal, QC, Canada, 2014.

[25] W. Situ, G. Zhang, X. Li et al., "A thermal management system for rectangular $LiFePO_4$ battery module using novel double copper mesh-enhanced phase change material plates," *Energy*, vol. 141, pp. 613–623, 2017.

[26] C.-W. Zhang, K.-J. Xu, L.-Y. Li, M.-Z. Yang, H.-B. Gao, and S.-R. Chen, "Study on a battery thermal management system based on a thermoelectric effect," *Energies*, vol. 11, no. 2, 2018.

[27] Y. M. Seo, M. Y. Ha, S. H. Park, G. H. Lee, Y. S. Kim, and Y. G. Park, "A numerical study on the performance of the thermoelectric module with different heat sink shapes," *Applied Thermal Engineering*, vol. 128, pp. 1082–1094, 2018.

[28] W. He, G. Zhang, X. X. Zhang, J. Ji, G. Q. Li, and X. D. Zhao, "Recent development and application of thermoelectric generator and cooler," *Applied Energy*, vol. 143, pp. 1–25, 2015.

[29] X. H. Yang, S. C. Tan, and J. Liu, "Thermal management of Li-ion battery with liquid metal," *Energy Conversion and Management*, vol. 117, pp. 577–585, 2016.

[30] A. M. Sefidan, A. Sojoudi, and S. C. Saha, "Nanofluid-based cooling of cylindrical lithium-ion battery packs employing forced air flow," *International Journal of Thermal Sciences*, vol. 117, pp. 44–58, 2017.

[31] T. H. Tran, S. Harmand, and B. Sahut, "Experimental investigation on heat pipe cooling for hybrid electric vehicle and electric vehicle lithium-ion battery," *Journal of Power Sources*, vol. 265, pp. 262–272, 2014.

[32] K. Shah, C. McKee, D. Chalise, and A. Jain, "Experimental and numerical investigation of core cooling of Li-ion cells using heat pipes," *Energy*, vol. 113, pp. 852–860, 2016.

[33] S. Wilke, B. Schweitzer, S. Khateeb, and S. al-Hallaj, "Preventing thermal runaway propagation in lithium ion battery packs using a phase change composite material: an experimental study," *Journal of Power Sources*, vol. 340, pp. 51–59, 2017.

[34] G. Jiang, J. Huang, M. Liu, and M. Cao, "Experiment and simulation of thermal management for a tube-shell Li-ion battery pack with composite phase change material," *Applied Thermal Engineering*, vol. 120, pp. 1–9, 2017.

[35] Q. Wang, B. Jiang, B. Li, and Y. Y. Yan, "A critical review of thermal management models and solutions of lithium-ion batteries for the development of pure electric vehicles," *Renewable and Sustainable Energy Reviews*, vol. 64, pp. 106–128, 2016.